



Recombinant Isfahan Virus and Vesicular Stomatitis Virus Vaccine Vectors Provide Durable, Multivalent, Single-Dose Protection against Lethal Alphavirus Challenge

Farooq Nasar,^{a*} Demetrius Matassov,^b Robert L. Seymour,^a Theresa Latham,^b Rodion V. Gorchakov,^c Rebecca M. Nowak,^b Grace Leal,^a Stefan Hamm,^b John H. Eldridge,^b Robert B. Tesh,^a David K. Clarke,^b Scott C. Weaver^a

Institute for Human Infections and Immunity, Center for Tropical Diseases, and Departments of Pathology and Microbiology and Immunology, University of Texas Medical Branch, Galveston, Texas, USA^a; Profectus BioSciences Inc., Tarrytown, New York, USA^b; Department of Pediatrics, Section of Tropical Medicine, Baylor College of Medicine, Houston, Texas, USA^c

ABSTRACT The demonstrated clinical efficacy of a recombinant vesicular stomatitis virus (rVSV) vaccine vector has stimulated the investigation of additional serologically distinct *Vesiculovirus* vectors as therapeutic and/or prophylactic vaccine vectors to combat emerging viral diseases. Among these viral threats are the encephalitic alphaviruses Venezuelan equine encephalitis virus (VEEV) and Eastern equine encephalitis virus (EEEV), which have demonstrated potential for natural disease outbreaks, yet no licensed vaccines are available in the event of an epidemic. Here we report the rescue of recombinant Isfahan virus (rISFV) from genomic cDNA as a potential new vaccine vector platform. The rISFV genome was modified to attenuate virulence and express the VEEV and EEEV E2/E1 surface glycoproteins as vaccine antigens. A single dose of the rISFV vaccine vectors elicited neutralizing antibody responses and protected mice from lethal VEEV and EEEV challenges at 1 month postvaccination as well as lethal VEEV challenge at 8 months postvaccination. A mixture of rISFV vectors expressing the VEEV and EEEV E2/E1 glycoproteins also provided durable, single-dose protection from lethal VEEV and EEEV challenges, demonstrating the potential for a multivalent vaccine formulation. These findings were paralleled in studies with an attenuated form of rVSV expressing the VEEV E2/E1 glycoproteins. Both the rVSV and rISFV vectors were attenuated by using an approach that has demonstrated safety in human trials of an rVSV/HIV-1 vaccine. Vaccines based on either of these vaccine vector platforms may present a safe and effective approach to prevent alphavirus-induced disease in humans.

IMPORTANCE This work introduces rISFV as a novel vaccine vector platform that is serologically distinct and phylogenetically distant from VSV. The rISFV vector has been attenuated by an approach used for an rVSV vector that has demonstrated safety in clinical studies. The vaccine potential of the rISFV vector was investigated in a well-established alphavirus disease model. The findings indicate the feasibility of producing a safe, efficacious, multivalent vaccine against the encephalitic alphaviruses VEEV and EEEV, both of which can cause fatal disease. This work also demonstrates the efficacy of an attenuated rVSV vector that has already demonstrated safety and immunogenicity in multiple HIV-1 phase I clinical studies. The absence of serological cross-reactivity between rVSV and rISFV and their phylogenetic divergence within the *Vesiculovirus* genus indicate potential for two stand-alone vaccine

Received 5 September 2016 Accepted 12 January 2017

Accepted manuscript posted online 1 February 2017

Citation Nasar F, Matassov D, Seymour RL, Latham T, Gorchakov RV, Nowak RM, Leal G, Hamm S, Eldridge JH, Tesh RB, Clarke DK, Weaver SC. 2017. Recombinant Isfahan virus and vesicular stomatitis virus vaccine vectors provide durable, multivalent, single-dose protection against lethal alphavirus challenge. *J Virol* 91:e01729-16. <https://doi.org/10.1128/JVI.01729-16>.

Editor Stanley Perlman, University of Iowa

Copyright © 2017 American Society for Microbiology. All Rights Reserved.

Address correspondence to Farooq Nasar, fanasar@icloud.com, or Scott C. Weaver, sweaver@utmb.edu.

* Present address: Farooq Nasar, Virology Division, United States Army Medical Research Institute of Infectious Diseases, Frederick, Maryland, USA.

vector platforms that could be used to target multiple bacterial and/or viral agents in successive immunization campaigns or as heterologous prime-boost agents.

KEYWORDS Eastern equine encephalitis virus, Isfahan virus, Venezuelan equine encephalitis virus, vesicular stomatitis virus

The genus *Vesiculovirus* in the family *Rhabdoviridae* consists of arthropod-borne viruses that are transmitted to susceptible vertebrate hosts through insect bites (1). This genus consists of nine recognized virus species, including the prototypic species vesicular stomatitis virus (VSV) and Isfahan virus (ISFV) (2). ISFV was isolated from phlebotomine sandflies in Dormian, Isfahan Province, Iran, in 1975 and is endemic in parts of Asia, including Iran, Turkmenistan, and the central Asian republics (3–5). Transmission to susceptible hosts occurs via biting insects, most likely sandflies, and although data indicate that ISFV can infect humans and domesticated animals, the infection has not been linked to any illness (3, 6).

VSV is found only in the Americas and is an important pathogen of domesticated animals, mainly ungulates (1). The virus was first reported during an outbreak in cattle and horses in 1916 and was subsequently isolated from cattle in 1925 in Richmond, IN (7). Infection in animals causes vesicular lesions at insect bite sites around the mouth, nose, teats, and coronary bands on the hooves (8). The vesicular lesions may result in lameness and weight loss due to difficulty in feeding but typically resolve in 7 to 10 days without serious consequences (8). Humans can also be infected with VSV at mucosal surfaces as a result of either close contact with infected animals or accidental exposure in the laboratory (9, 10). The resulting infection may either be subclinical or produce mild flu-like symptoms that typically resolve in 5 to 7 days without complications.

As a prototype member of the genus *Vesiculovirus*, VSV has been extensively studied, providing insights into many aspects of the virus replication cycle and shedding light on the biology of other related viruses. The VSV and ISFV genomes consist of a nonsegmented, single-strand, negative-sense RNA ~11 kb in length containing five genes in the order 3'-N-P-M-G-L-5', encoding the N, P, M, G, and L proteins, respectively (1, 11). The VSV particles are bullet-shaped (~80 nm by ~200 nm) and comprise a ribonucleoprotein core of genomic RNA and N (nucleocapsid) protein surrounded by a matrix (M) protein layer, enveloped by the host cell plasma membrane containing the transmembrane viral glycoprotein (G) (12). The phosphoprotein (P) and large (L) polymerase protein associate to form the functional viral RNA polymerase, which performs both mRNA transcription and genome replication from the nucleocapsid template (13, 14). Viral mRNA transcription initiates at the 3' end of the genome and proceeds with a pronounced 3'-to-5' gradient of gene expression, leading to abundant N protein and successively decreasing levels of P, M, G, and L proteins in the infected cell, providing virus proteins an optimal ratio for subsequent viral genome replication and the assembly of mature virus particles (11, 15). Virus replication *in vitro* is rapid, and virus progeny are detectable at 5 to 6 hours postinfection (hpi) in vertebrate cell lines.

The genomes of negative-strand viruses remained refractory to genetic manipulation until 1994, when the recovery of infectious rabies virus from viral genomic cDNA became possible (16). The development of similar rescue systems for other negative-strand viruses, including vesicular stomatitis Indiana virus (VSIV), followed quickly (17, 18). The ability to manipulate the VSIV genome enabled the development of recombinant VSIV (rVSIV) as a vaccine vector (19). The immunogenicity and protective efficacy of rVSIV vaccine vectors have been demonstrated for a range of human pathogens, including influenza virus, human immunodeficiency virus (HIV), herpes simplex virus 2 (HSV-2), respiratory syncytial virus (RSV), severe acute respiratory syndrome-associated coronavirus (SARS-CoV), chikungunya virus (CHIKV), and Ebola virus (EBOV), in small-animal and nonhuman primate (NHP) disease models (20–31). However, the safety of rVSIV vectors initially was a concern because both VSIV and the New Jersey serotype of VSV (vesicular stomatitis New Jersey virus [VSNJV]) are known to have neurotropic

properties in young mice and can cause neurological disease following intracranial (i.c.) inoculation of cows and horses (32–35). A pilot NHP neurovirulence (NV) study indicated that a prototypic rVSV vector was insufficiently attenuated for clinical evaluation (36–38). To reduce NV potential and enhance vector safety, a variety of attenuation strategies were devised and tested in animal disease models (39–41). The most promising strategy was a combination of N gene translocation with a truncation of the cytoplasmic tail (CT) of the G protein, enabling a very marked reduction of NV in young mice. One of the most highly attenuated vectors (rVSV-N4CT1HIVgag1) produced little evidence of injury in the central nervous system (CNS) when NHPs were inoculated by the intrathalamic route yet elicited an immune response that was similar to those induced by more virulent vectors when inoculated by the intramuscular (i.m.) route (39). These preclinical studies supported the evaluation of rVSV-N4CT1HIVgag1 in recently concluded phase I human clinical trials (HVTN 090 and HVTN 087), where the rVSV vector demonstrated safety at a dose as high as 10^8 PFU and immunogenicity at a dose as low as 10^4 PFU (42).

An important target of biodefense vaccines are members of the genus *Alphavirus* of the family *Togaviridae*, which is comprised of small, spherical, enveloped viruses with genomes consisting of a single-strand, positive-sense RNA 11 to 12 kb in length (1). Alphaviruses comprise 31 recognized species classified into 11 complexes based on antigenic and/or genetic similarities (43, 44). The two aquatic alphavirus complexes are not known to utilize arthropods in their transmission cycles, whereas all of the remaining complexes (Barmah Forest virus, Ndumu virus, Middelburg virus, Semliki Forest virus, Venezuelan equine encephalitis virus [VEEV], Eastern equine encephalitis virus [EEEV], Western equine encephalitis virus [WEEV], Trocara virus, and Eilat virus) consist of arboviruses that almost exclusively utilize mosquitoes as vectors (1, 45–47). Mosquito-borne alphaviruses infect diverse vertebrate hosts, including equids, birds, amphibians, reptiles, rodents, pigs, humans, and NHPs (1). The ability to infect both mosquitoes and vertebrates enables the maintenance of alphaviruses in natural endemic transmission cycles that occasionally spill over into the human population and cause disease. Infection with Old World alphaviruses such as CHIKV, o'nyong-nyong virus (ONNV), Sindbis virus (SINV), and Ross River virus (RRV) are rarely fatal, and disease is characterized by rash and debilitating arthralgia that can persist for months or years. In contrast, New World alphaviruses such as WEEV, EEEV, and VEEV can cause fatal encephalitis. Human case fatality rates for EEEV range from 40 to 80%, whereas those for WEEV and VEEV infections range from <1 to 5% (1). In addition, all three viruses are lethal (EEEV and WEEV) or highly debilitating (VEEV) in NHPs after aerosol infection (48–50). Currently, there are no licensed antiviral treatments or vaccines for alphaviral diseases, and the U.S. population remains vulnerable to natural disease outbreaks.

Here we report the first recovery of infectious rISFV from genomic cDNA and demonstrate the immunogenicity and protective efficacy of attenuated forms of rISFV and rVSV vector vaccines in mouse models of VEEV- and EEEV-induced disease.

RESULTS

Genetic and phylogenetic analysis of ISFV. The available N, G, and L gene sequences of currently recognized and tentatively classified members of the genus *Vesiculovirus* were downloaded from GenBank and aligned (Table 1). Genetic analysis was performed by comparing both nucleotide and deduced amino acid sequences (Tables 2 to 4). Nucleotide and amino acid sequence identities of the ISFV genes with other members of the genus ranged from 48 to 65% and 37 to 69%, respectively. Isfahan virus genes consistently had higher nucleotide and amino acid sequence identities with Chandipura virus (CHNV), Malpais Springs virus (MSPV), and Jurona virus (JURV) than with VSIV, with N gene nucleotide and amino acid identities that were 2 to 8% and 6 to 14% higher, G gene nucleotide and amino acid identities that were 5 to 9% and 10 to 14% higher, and L gene nucleotide and amino acid identities that were 5 to 6% and 8 to 11% higher, respectively (Tables 2 to 4).

TABLE 1 List of rhabdovirus sequences utilized in analyses

| Species | Abbreviation | GenBank accession no. |
|---------------------------------------|--------------|-----------------------|
| Carajas virus | CARAV | HW243161 |
| Chandipura virus | CHNV | GU212858 |
| Cocal virus | COCV | EU373657 |
| Isfahan virus | ISFV | AJ810084 |
| Jurona virus | JURV | HM566194 |
| Malpais Spring virus | MSPV | KC412247 |
| Maraba virus | MARV | HQ660076 |
| Perinet virus | PERV | HM566195 |
| Piry virus | PIRV | D26175 |
| Vesicular stomatitis Alagoas virus | VSAV | EU373658 |
| Vesicular stomatitis Indiana virus | VSIV | NC_001560 |
| Vesicular stomatitis New Jersey virus | VSNJV | NC_024473 |

Phylogenetic trees were generated by utilizing the maximum likelihood (ML) method to study the evolutionary relatedness between ISFV and other vesiculoviruses. Based on comparisons of N, G, and L gene nucleotide sequences, the phylogenetic analysis revealed similar evolutionary relationships. Two branching patterns were observed: one main branch consisted of VSIV, its subtypes, and VSNJV, and another branch consisted of ISFV, CHNV, JURV, Perinet virus (PERV), Piry virus (PIRV), and MSPV (Fig. 1). Major branching nodes were statistically supported with bootstrap values of 100% in both analyses; however, statistical support for internal nodes was limited (Fig. 1). These analyses showed that ISFV is more closely related to CHNV, JURV, PERV, PIRV, and MSPV than to VSIV and VSNJV.

In vitro characterization of wild-type ISFV and VSIV. The plaque phenotype and one-step replication kinetics of wild-type (wt) isolates of ISFV and the VSIV San Juan strain were compared (see Fig. 4B and C). Both isolates displayed similar plaque phenotypes, reaching ~3 to 4 mm in diameter at 48 hpi, and replication kinetics in Vero cell monolayers were almost identical, with peak titers of 5×10^8 PFU/ml being achieved at 6 to 12 hpi.

Generation of rISFV. The assembly of a full-length rISFV genomic cDNA and plasmids expressing the ISFV N, P, M, G, and L proteins was carried out in a manner similar to that used previously for the generation of rVSIV and mumps virus (MuV) genomic cDNAs (16–18, 51). High-efficiency rescue of infectious rISFV from genomic cDNA was achieved by the electroporation of Vero cells with plasmids encoding full-length genomic cDNA and the N, P, M, G, and L proteins as described previously for the rescue of rVSIV and other negative-strand RNA viruses (Fig. 2B) (52). The recovery of rISFV was indicated by the induction of cytopathic effects (CPE) in Vero cells upon passaging of the transfected cell supernatant onto fresh monolayers and confirmed by full-length genomic sequencing of the resulting virus progeny. rISFV displayed a plaque phenotype (~3 to 4 mm in diameter at 48 hpi), replication kinetics, and

TABLE 2 Nucleotide and amino acid comparison based on full-length N gene sequences of members of the genus *Vesiculovirus*^a

| Virus | % sequence identity in N gene | | | | | | | | |
|-------|-------------------------------|-----------|-----------|-----------|-----------|-----------|-----------|-----------|-----------|
| | ISFV | CHNV | MSPV | JURV | VSIV | VSAV | COCV | MARV | VSNJV |
| ISFV | | 58 | 65 | 66 | 52 | 52 | 51 | 51 | 52 |
| CHNV | 59 | | 58 | 61 | 50 | 48 | 48 | 50 | 50 |
| MSPV | 64 | 61 | | 70 | 56 | 55 | 55 | 56 | 56 |
| JURV | 65 | 62 | 65 | | 54 | 55 | 53 | 53 | 54 |
| VSIV | 56 | 55 | 58 | 57 | | 85 | 84 | 90 | 69 |
| VSAV | 57 | 55 | 57 | 54 | 73 | | 85 | 83 | 69 |
| COCV | 55 | 55 | 57 | 56 | 74 | 74 | | 87 | 70 |
| MARV | 54 | 56 | 56 | 56 | 76 | 75 | 76 | | 70 |
| VSNJV | 56 | 56 | 58 | 56 | 69 | 66 | 66 | 66 | |

^aPercent nucleotide identity is shown below the diagonal in lightface type. Percent amino acid identity is shown above the diagonal in boldface type.

TABLE 3 Nucleotide and amino acid comparison based on full-length G gene sequences of members of the genus *Vesiculovirus*^a

| Virus | % sequence identity in G gene | | | | | | | | | | |
|-------|-------------------------------|-----------|-----------|-----------|-----------|-----------|-----------|-----------|-----------|-----------|-----------|
| | ISFV | CHNV | MSPV | JURV | PIRV | PERV | VSIV | VSAV | COCV | MARV | VSNJV |
| ISFV | | 54 | 49 | 54 | 50 | 50 | 39 | 37 | 41 | 39 | 38 |
| CHNV | 56 | | 48 | 52 | 51 | 51 | 39 | 40 | 39 | 40 | 37 |
| MSPV | 54 | 53 | | 49 | 48 | 49 | 36 | 37 | 37 | 36 | 37 |
| JURV | 58 | 57 | 54 | | 49 | 51 | 37 | 37 | 38 | 37 | 37 |
| PIRV | 55 | 55 | 55 | 56 | | 57 | 39 | 38 | 38 | 39 | 37 |
| PERV | 55 | 56 | 55 | 56 | 60 | | 38 | 40 | 38 | 39 | 38 |
| VSIV | 49 | 47 | 46 | 48 | 48 | 46 | | 63 | 71 | 77 | 49 |
| VSAV | 48 | 49 | 47 | 48 | 48 | 49 | 64 | | 66 | 64 | 48 |
| COCV | 49 | 47 | 46 | 48 | 47 | 46 | 69 | 65 | | 73 | 47 |
| MARV | 49 | 48 | 45 | 48 | 48 | 48 | 71 | 65 | 69 | | 50 |
| VSNJV | 48 | 48 | 47 | 49 | 47 | 46 | 55 | 55 | 53 | 55 | |

^aPercent nucleotide identity is shown below the diagonal in lightface type. Percent amino acid identity is shown above the diagonal in boldface type.

a peak titer ($\sim 3 \times 10^8$ PFU/ml) similar to those of wt ISFV (see Fig. 4B and C). These findings confirmed the recovery of infectious rISFV from genomic cDNA and created a pathway for further modification of rISFV as a vaccine vector.

In vitro characterization of rISFV and rVSIV vectors encoding alphavirus antigens. Both the rISFV and rVSIV vectors were altered to express alphavirus E3-E2-6k/TF-E1 (E3-E1) antigens. The E3-E1 genes of the North American lineage of EEEV strain FL93-939 and VEEV subtype ID strain ZPC 738 (VEEV-ID), were inserted into the fifth position of the rISFV genome(s) (Fig. 3), which also had the N gene translocated to position 4 (Fig. 3), a strategy that was successful in attenuating rVSIV replication *in vitro* (35, 40, 53, 54). In addition, an rVSIV-N4CT1 vector, very similar in design to the vector which demonstrated safety and immunogenicity in phase I clinical trials, was also modified to express the VEEV-ID E3-E1 genes in the fifth position of the genome (Fig. 3) (42).

All three vectors were characterized *in vitro* for the expression of alphavirus antigens, plaque phenotype, and replication kinetics in Vero cells (Fig. 3 and 4); the rISFV and rVSIV vectors demonstrated robust alphavirus antigen expression, displayed a small-plaque phenotype (~ 1 to 2 mm in diameter at 72 hpi compared to ~ 3 to 4 mm at 48 hpi for wt viruses), and a significant reduction in replication efficiency (~ 10 - to 10,000-fold at 12 to 48 hpi) relative to those of unaltered rISFV or rVSIV-HIV (Fig. 4A to C). These data indicated that, like rVSIV, rISFV can also be attenuated by N gene shuffling and that both the attenuated rISFV and rVSIV vectors can express abundant alphavirus antigens while achieving peak titers of $\sim 10^6$ PFU/ml on Vero cell monolayers.

TABLE 4 Nucleotide and amino acid comparison based on full-length L gene sequences of members of the genus *Vesiculovirus*^a

| Virus | % sequence identity in L gene | | | | | | | | | | |
|-------|-------------------------------|-----------|-----------|-----------|-----------|-----------|-----------|-----------|-----------|-----------|-----------|
| | ISFV | CHNV | MSPV | JURV | PERV | CARV | VSIV | VSAV | COCV | MARV | VSNJV |
| ISFV | | 69 | 69 | 66 | 67 | 59 | 58 | 58 | 58 | 59 | 58 |
| CHNV | 64 | | 68 | 67 | 66 | 59 | 59 | 58 | 58 | 59 | 58 |
| MSPV | 63 | 63 | | 68 | 67 | 59 | 59 | 59 | 59 | 59 | 58 |
| JURV | 63 | 63 | 63 | | 64 | 59 | 58 | 58 | 58 | 58 | 58 |
| PERV | 63 | 62 | 63 | 62 | | 59 | 57 | 58 | 58 | 57 | 57 |
| CARV | 58 | 59 | 59 | 58 | 59 | | 70 | 70 | 69 | 69 | 70 |
| VSIV | 58 | 58 | 59 | 58 | 57 | 65 | | 76 | 77 | 78 | 66 |
| VSAV | 58 | 58 | 58 | 58 | 58 | 64 | 67 | | 78 | 77 | 67 |
| COCV | 58 | 58 | 59 | 58 | 59 | 64 | 69 | 69 | | 79 | 66 |
| MARV | 58 | 59 | 58 | 58 | 58 | 64 | 69 | 68 | 69 | | 66 |
| VSNJV | 59 | 58 | 59 | 58 | 58 | 66 | 63 | 63 | 63 | 63 | |

^aPercent nucleotide identity is shown below the diagonal in lightface type. Percent amino acid identity is shown above the diagonal in boldface type.

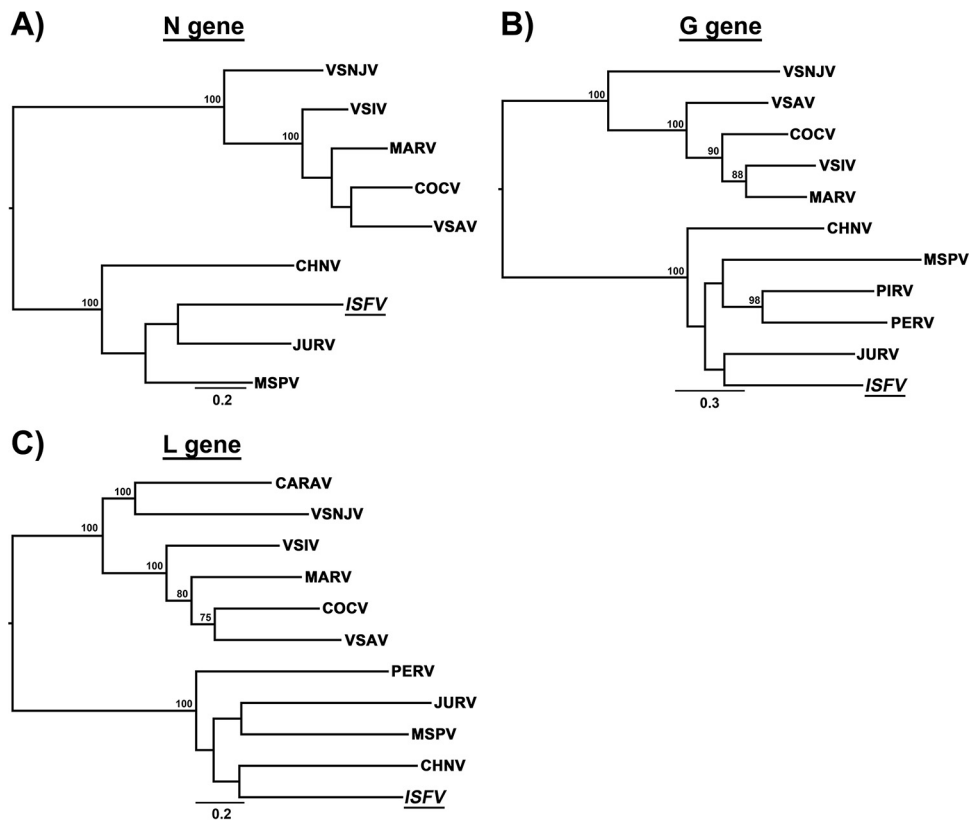


FIG 1 Midpoint-rooted maximum likelihood tree based on nucleotide sequences of the N, G, and L genes. Bootstrap values of $>75\%$ are shown at internal nodes. The bar represents nucleotide substitutions per site.

Assessment of rISFV vaccine vector efficacy. The efficacy of both rISFV-VEEV and EEEV vaccine candidates was assessed by lethal alphavirus challenge in a murine model. Cohorts of 10 CD-1 mice were vaccinated i.m. with 10^8 PFU/mouse of rISFV-VEEV or with a sham vaccine (Fig. 5). At 4 weeks postvaccination, animals were challenged subcutaneously (s.c.) with 10^4 PFU/mouse of VEEV-ID. Weight loss was observed by as early as 2 days postchallenge in sham-vaccinated animals and increased to $>20\%$ of the starting body mass at the time of euthanasia (Fig. 5B). By day 8 postchallenge, all mice showed signs of severe illness and met euthanasia criteria (Fig. 5C). In contrast, no weight loss or other signs of disease or lethality were observed in vaccinated mice (Fig. 5B and C).

Similarly to the rISFV-VEEV study, cohorts of CD-1 mice were either sham vaccinated or vaccinated i.m. with 10^8 PFU/mouse of rISFV-EEEV (Fig. 6A). Neutralizing antibody responses were measured via an 80% plaque reduction neutralization titer (PRNT₈₀) test at 14 and 21 days postvaccination (Fig. 6A). All sham-vaccinated mice remained seronegative (PRNT₈₀ of <20), whereas 80% and 100% of the vaccinated mice had a PRNT₈₀ of ≥ 20 at 14 and 21 days postvaccination, respectively (Fig. 6B). At 28 days postvaccination, mice were challenged s.c. with 10^4 PFU/mouse of EEEV (Fig. 6A). Sham-vaccinated mice lost weight beginning at day 5 postchallenge, continuing until euthanasia criteria were met (Fig. 6C). Similarly to previous studies, weight loss was not as pronounced as that with VEEV challenge, occurring closer to the time of euthanasia, which was performed once mice became moribund. Nonetheless, the sham-vaccinated mice succumbed to disease starting at day 6 postchallenge, and 60% met euthanasia criteria (Fig. 6D), while none of the vaccinated mice showed any signs of disease. These data demonstrated that an attenuated rISFV vector(s) expressing E3-E1 antigens could protect mice against lethal VEEV and EEEV challenges following a single i.m. vaccination.

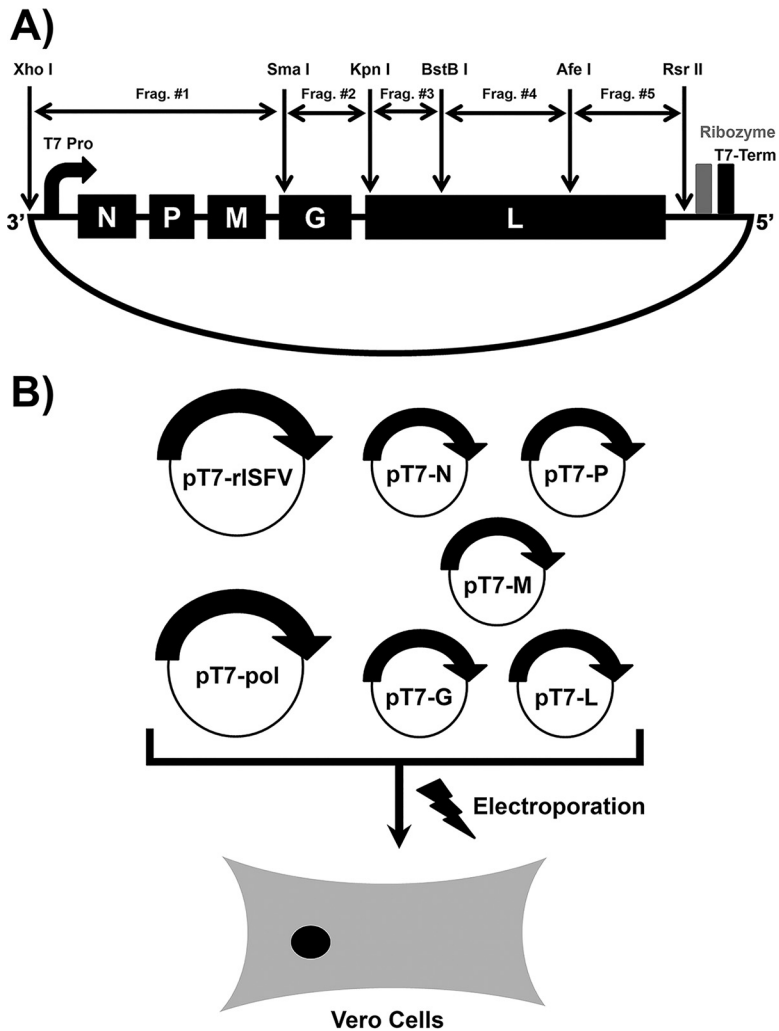


FIG 2 (A) Schematic diagram of the strategy utilized to generate the rISFV genomic cDNA clone. The full-length viral genome was cloned in 5 fragments flanked by unique restriction sites. The 3' leader and 5' trailer were flanked by the T7 RNA polymerase promoter and terminator, respectively. The hepatitis delta virus ribozyme sequence was used to generate a precise 5' trailer nucleotide sequence. (B) Outline of a helper-virus-free method of rescuing infectious rISFV. The T7 RNA polymerase and full-length and support rISFV plasmids were electroporated into Vero cells, and infectious virus was recovered at 5 to 10 days postelectroporation.

Efficacy of bivalent rISFV-VEEV and -EEEV vaccines against lethal alphavirus challenge. To assess the ability of rISFV vectors to provide protection against multiple alphaviruses, the rISFV-VEEV and -EEEV vectors were blended into a bivalent formulation, and cohorts of 20 CD-1 mice (VEEV) or 21 CD-1 mice (EEEV) were either sham vaccinated or vaccinated i.m. with 10^8 PFU/mouse of each vector, followed by lethal VEEV and EEEV challenges (10 mice [VEEV] or 11 mice [EEEV] per challenge virus) (Fig. 7A). The neutralizing antibody response was measured via a PRNT₈₀ assay at 14 and 21 days postvaccination. Similarly to the study described above, VEEV PRNT₈₀ titers of ≥ 20 were detected in 60% and 80% of mice at days 14 and 21 postvaccination, respectively (Fig. 7B). EEEV-neutralizing antibody responses were also detected at both time points in all mice, whereas all sham-vaccinated mice had PRNT₈₀ values below the limit of detection (Fig. 7B). Following VEEV challenge, all 10 sham-vaccinated mice succumbed to infection and were euthanized within 7 days of challenge, while vaccinated mice remained free of detectable disease (Fig. 7C). Sensitivity to lethal EEEV infection was increased by challenging mice with 10^5 PFU/mouse via the intraperitoneal (i.p.) route. Following EEEV challenge, the majority (9/11 animals) of sham-vaccinated mice suc-

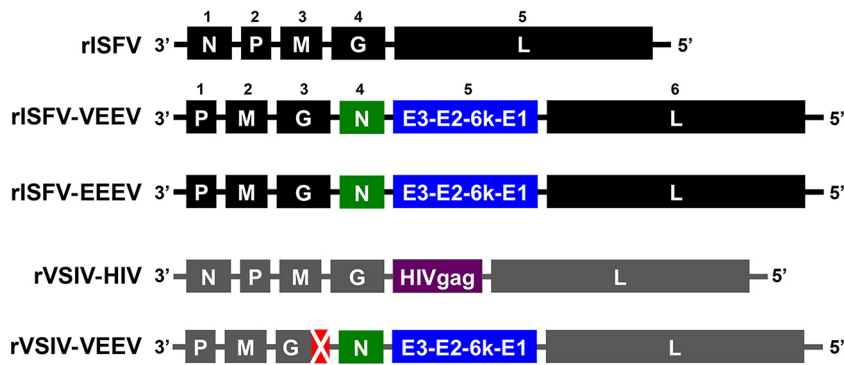


FIG 3 Schematic diagrams of the genetic organization and nomenclature of rISFV and rVSIV vectors. The N gene of rISFV-VEEV, rISFV-EEEV, and rVSIV-VEEV vectors was relocated to the fourth position of the genome. The rVSIV-VEEV vector also has a 28-amino-acid truncation in the cytoplasmic tail of the G protein. All foreign gene expression cassettes were added at genome position 5.

cumbed to infection and were euthanized within 7 days of challenge, while vaccinated mice remained free of detectable disease (Fig. 7C). These data demonstrated that a single dose of the blended rISFV-VEEV and -EEEV vaccines can provide complete protection from lethal VEEV and EEEV challenges.

Short- and long-term efficacies of rVSIV and rISFV vaccine vectors against lethal challenge. Short- and long-term protection induced by rISFV- and rVSIV-VEEV vectors was assessed by vaccinating cohorts of 10 CD-1 mice with 10^8 and 10^7 PFU/mouse of each vaccine vector, followed by lethal VEEV challenge at days 35 and 245 postvaccination (Fig. 8A and 9A). Antibody responses were measured via a PRNT₈₀ assay at days 25, 35, and 245 postvaccination. Neutralizing antibodies were detected in

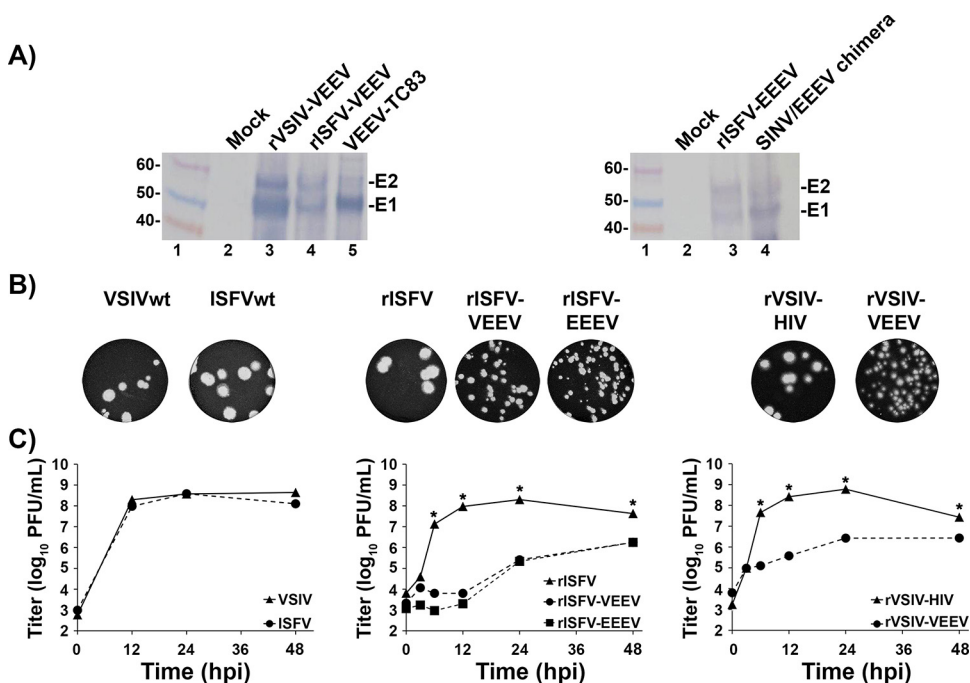


FIG 4 *In vitro* characterization of rISFV vectors. (A) Western blot analysis of rISFV and rVSIV vectors expressing VEEV or EEEV E3-E1 proteins in Vero cells. Replicate Vero cell monolayers in six-well plates were infected at an MOI of 5 PFU/cell, and cell lysates were collected at 24 hpi. The E3-E1 proteins were detected with mouse polyclonal antisera against VEEV and EEEV. (B and C) Plaque phenotype (B) and replication kinetics (C) of rISFV and rVSIV vectors in Vero cells. The plaque phenotype was assessed in Vero cell monolayers infected with wt ISFV, wt VSIV, rISFV, and rVSIV vectors, and at 2 to 3 days postinfection, the cells were fixed and stained with crystal violet. Assays of replication kinetics (C) of all viruses were performed at an MOI of 10 PFU/cell in triplicate. Average titers ± standard deviations (error bars) are shown. *, *P* values of <0.02.

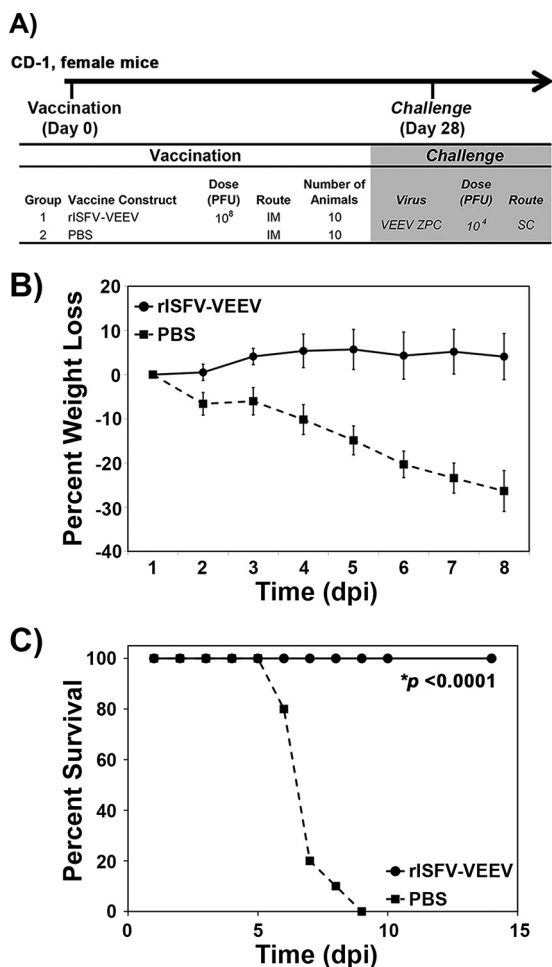


FIG 5 Efficacy of the rISFV-VEEV vector in CD-1 mice. (A) Outline of the study design. (B and C) Percent weight loss (B) and survival (C) following lethal VEEV-ID challenge via the s.c. route. Average weight loss \pm standard deviations (error bars) are shown. dpi, days postinfection.

mice at all time points postvaccination regardless of the virus vector or dose. PRNT₈₀ values of ≥ 20 were detected in 80 to 100% of vaccinated mice, and titers were maintained for the duration of the study (Fig. 8B and 9B). Average PRNT₈₀ values induced by rISFV-VEEV following either dose at 25 and 35 days postvaccination ranged from 40 to 160 and were reduced to 25 to 64 at day 245 (Fig. 8B and 9B), while rVSV-VEEV-induced PRNT₈₀ titers ranged from 288 to 600 at days 25 and 35 postvaccination and 304 to 360 at day 245 postvaccination (Fig. 8B and 9B). All vaccinated mice challenged at day 35 or 245 postvaccination with a lethal VEEV dose were protected from disease by both vectors at both dose levels, whereas 100% (day 35) and 75% (day 245) of the sham-vaccinated mice succumbed to infection and were euthanized within 6 to 14 days of challenge (Fig. 8C and 9C). These data demonstrated that both the attenuated rISFV and rVSV vaccine vectors could elicit a durable neutralizing antibody response and provided single-dose short- and long-term protection against lethal VEEV challenge.

DISCUSSION

Various forms of rVSV have been developed as vaccine vectors and oncolytic agents, made possible by the pioneering work of John Rose and colleagues; one such highly attenuated rVSV vector recently demonstrated safety and immunogenicity in clinical trials (42, 55–61). Here we report the rescue of rISFV from cDNA, modification of the rISFV genome to attenuate potential virulence and to express VEEV and EEEV E3-E1

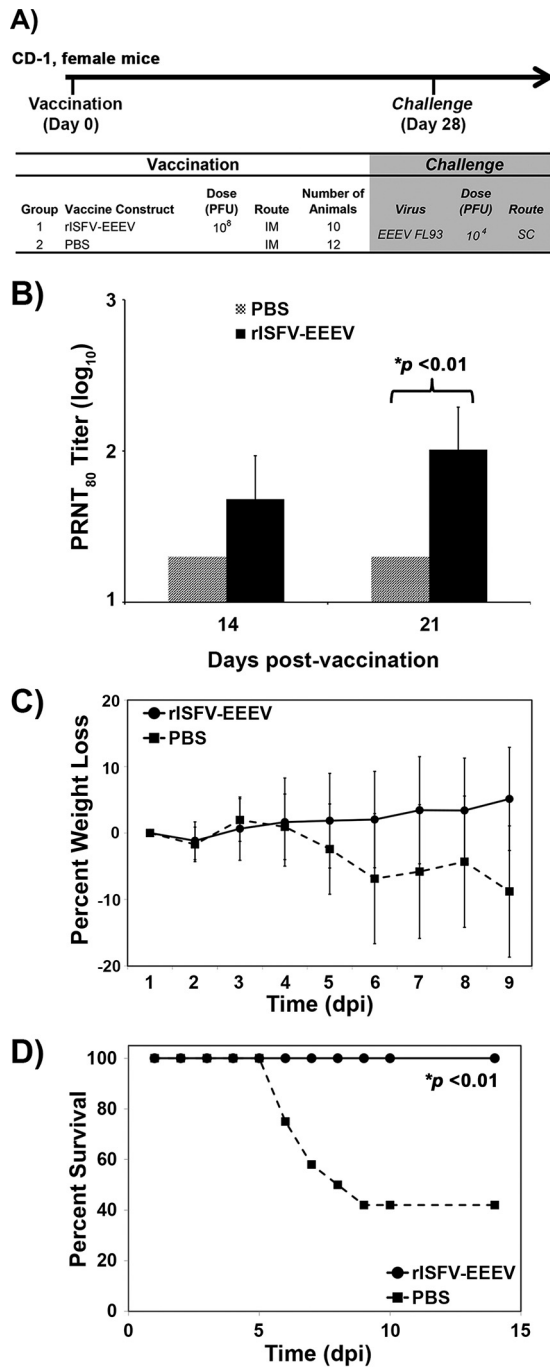


FIG 6 Immunogenicity and efficacy of the rISFV-EEEV vector in CD-1 mice. (A and B) Outline of the study design (A) and neutralizing antibody response measured by a PRNT₈₀ assay following rISFV-EEEV vaccination (B). (C and D) Percent weight loss (C) and survival (D) following lethal EEEV-NA challenge via the s.c. route. Average PRNT₈₀ values and weight loss ± standard deviations (error bars) are shown.

antigens, and the protective efficacy of the resulting rISFV vaccine vectors in lethal mouse models of VEEV and EEEV disease. A highly attenuated rVSIV vector, based on the rVSIV-N4CT1gag1 vector, which demonstrated safety and immunogenicity in phase I clinical trials, was also modified to express VEEV and EEEV E3-E1 antigens. This vaccine candidate was included in our studies as a comparator to the novel rISFV vector(s) and as a candidate stand-alone vaccine(s) to prevent alphavirus-induced disease.

The primary reasons for selecting ISFV as a potential vaccine vector were the

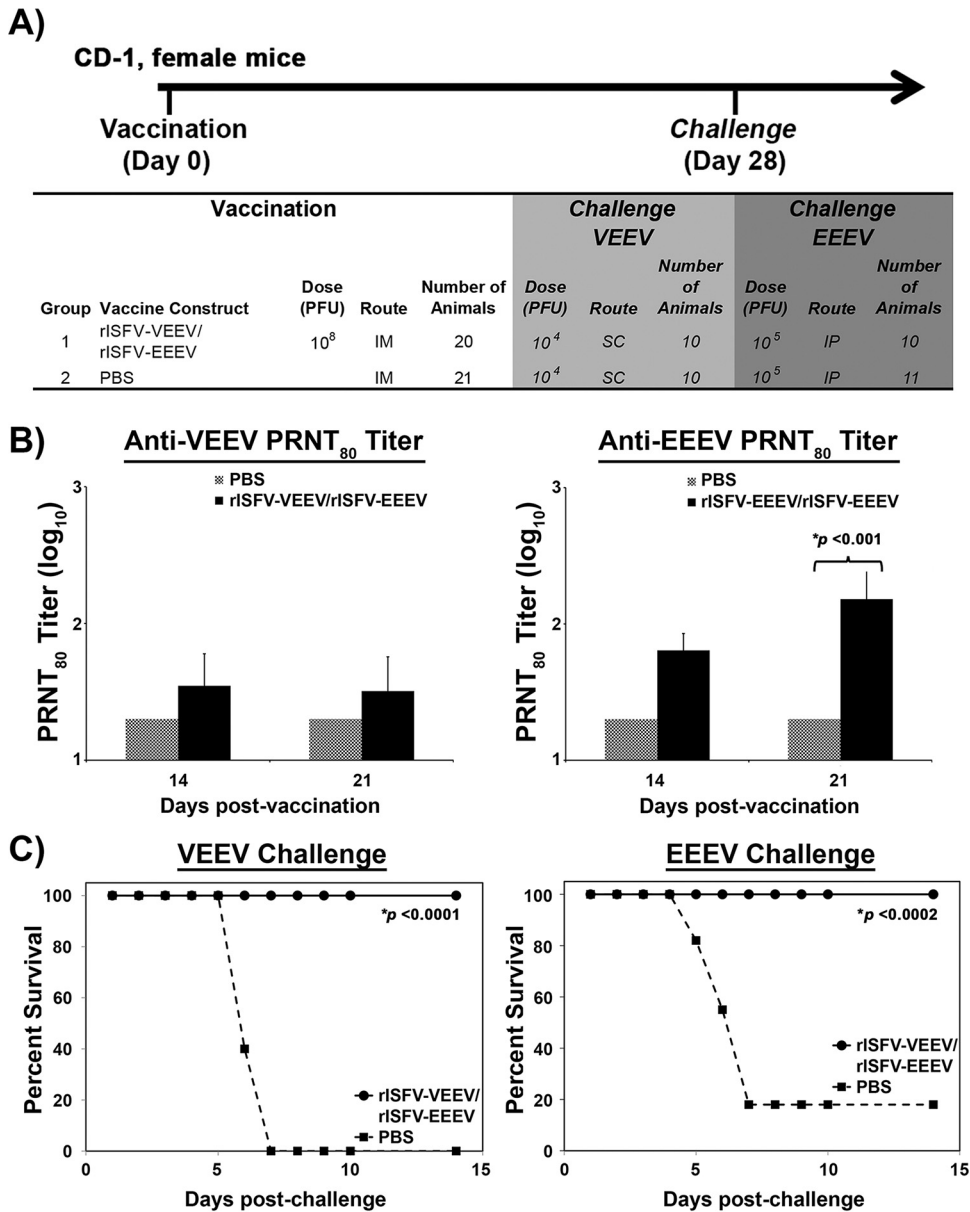


FIG 7 Immunogenicity and efficacy of blended rISFV-VEEV/rISFV-EEEV vectors. (A) Outline of the study design in CD-1 mice. (B) Neutralizing antibody response measured by a PRNT₈₀ assay following vaccination. (C) Survival following lethal VEEV-ID or EEEV-NA challenge via the s.c. or i.p. route, respectively. Average PRNT₈₀ values ± standard deviations (error bars) are shown.

phylogenetic distance from VSIV and known serological differences from VSIV and other vesiculoviruses (2, 3). The inability of serum from VSV-infected mice to neutralize ISFV and the divergence of the protein sequences between both viruses, reducing the likelihood of cross-reactive T cell epitopes, should allow rISFV vaccine vectors to elicit immune responses when used either as a booster after priming with rVSIV expressing autologous antigens or as a stand-alone vaccine vector for protection against heterologous disease to be used in people previously vaccinated with rVSIV vectors (2). The studies described here clearly demonstrate that rISFV vectors can be utilized as a stand-alone vaccine platform, and we are in the process of investigating the immunogenicity and protective efficacy of rISFV vectors in the context of preexisting rVSV immunity. Preliminary prime-boost studies with rVSV and rISFV vectors expressing an immunodominant HIV-1 Gag epitope suggest that immune responses elicited by rISFV vectors will not be blunted in mice with preexisting rVSIV immunity (our unpublished

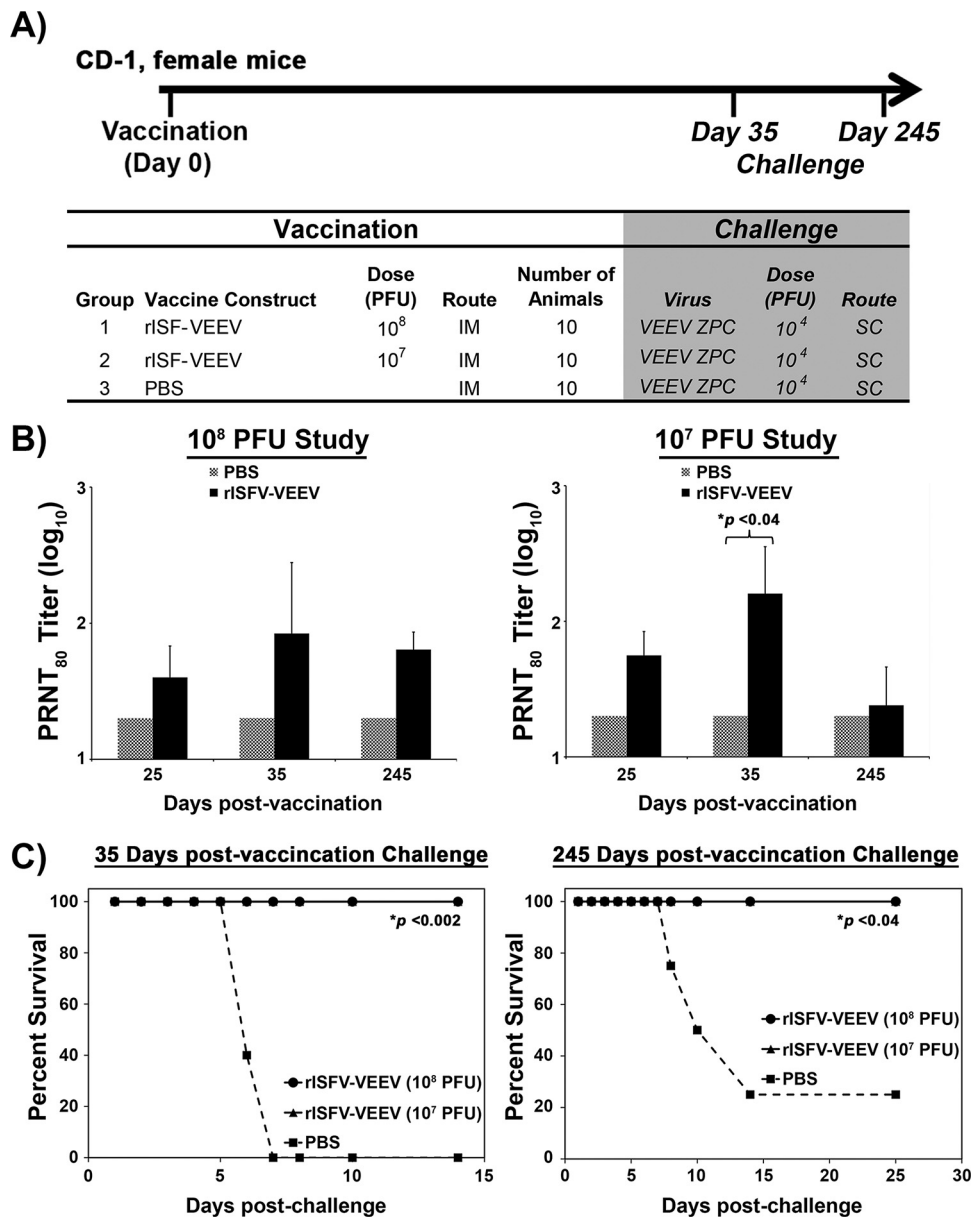


FIG 8 Dose titration and duration of efficacy of the rISFV-VEEV vector. (A) Outline of the study design in CD-1 mice. Animals were vaccinated with 10⁸ or 10⁷ PFU and challenged with lethal VEEV-ID at 35 and 245 days postinfection. (B) Neutralizing antibody response measured by a PRNT₈₀ assay following vaccination. (C) Survival following lethal VEEV-ID challenge via the s.c. route. Average PRNT₈₀ values ± standard deviations (error bars) are shown.

data). Also, preliminary neurovirulence studies in young mice indicated that unmodified wt ISFV was 1,000-fold more attenuated than wt VSIV, based on the amount of infectious virus required to provide a measurable 50% lethal dose (LD₅₀), presumably due to inherently lower-virulence properties and likely reducing the need for extensive attenuation compared to rVSV vectors (our unpublished data). The latter is also supported by the absence of any clinical signs of disease after vaccination of mice. The significance of this natural murine attenuation for humans is unknown, but greater sensitivity to innate immune responses *in vivo* could be responsible, given that unmodified rISFV and rVSV grew robustly and equally well in Vero cell monolayers. The anticipated safety of rISFV and attenuated rISFV vectors is supported by the seroconversion of people in regions of endemicity, presumably as a result of being bitten by an infected insect, without reported illness (3–5, 62).

The recovery of virus entirely from cDNA enabled the evaluation of rISFV as a new

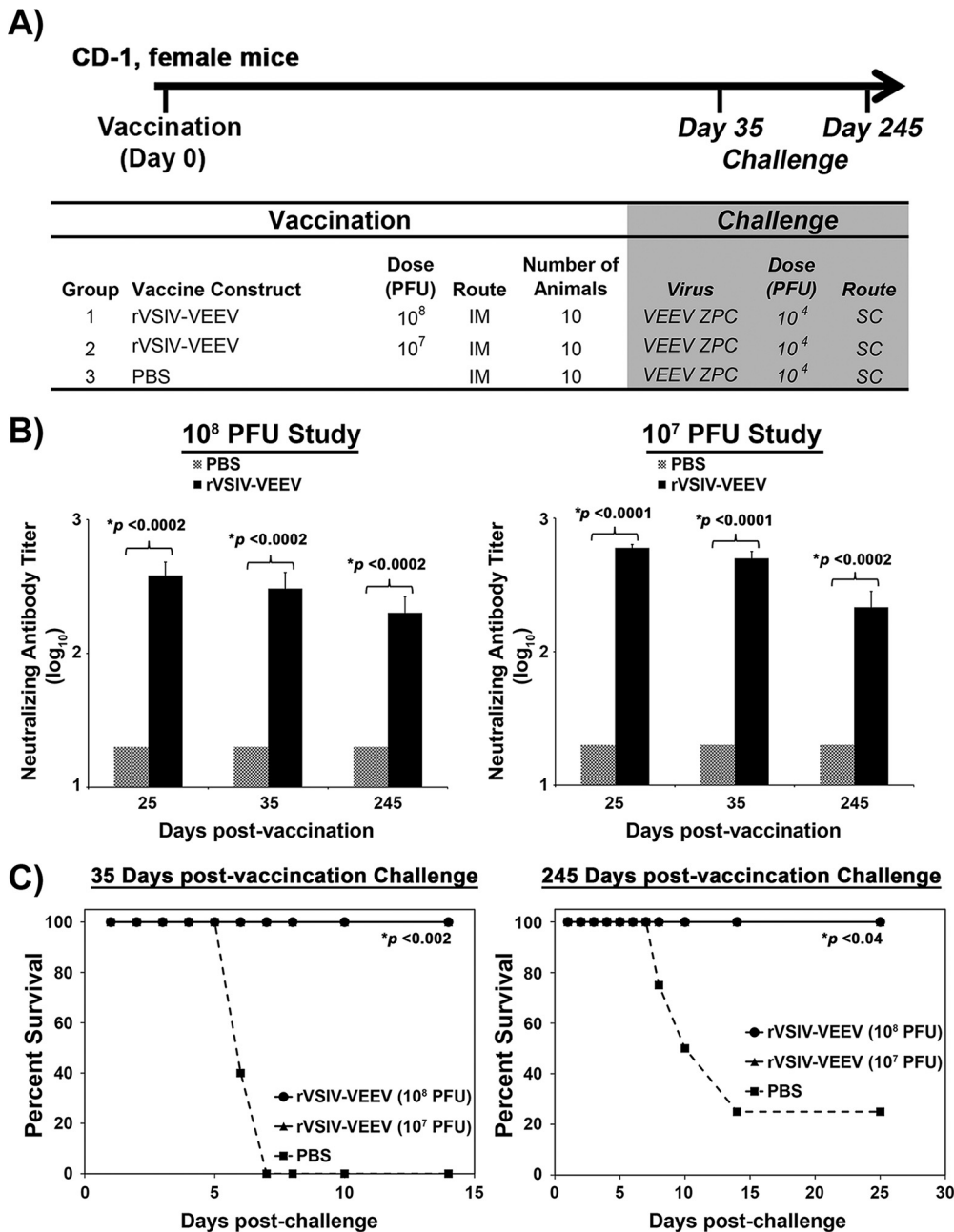


FIG 9 Dose titration and duration of efficacy of the rVSIV-VEEV vector. (A) Outline of the study design in CD-1 mice. Animals were vaccinated with 10⁸ or 10⁷ PFU and challenged with lethal VEEV-ID at 35 and 245 days postinfection. (B) Neutralizing antibody response measured by a PRNT₈₀ assay following vaccination. (C) Survival following lethal VEEV-ID challenge via the s.c. route. Average PRNT₈₀ values ± standard deviations (error bars) are shown.

vaccine vector. The alphaviruses VEEV and EEEV were selected as vaccine targets because both viruses cause serious and sometimes fatal disease in humans, and there are currently no licensed vaccines available to protect against either virus. Although rISFV was believed to be less virulent than rVSIV *in vivo* based on results from a preliminary neurovirulence study in young mice, additional attenuation was sought by N gene translocation, as previously reported for rVSIV (35, 40). The reduction of *in vitro* plaque sizes and the significant reduction in the level of progeny virus in replication kinetics studies indicated that moving the N gene to position 4 in the genome (N4) attenuates rISFV growth, although the potential contribution of VEEV/EEEV E3-E1 expression to attenuation was not formally tested. However, the shuffling of the rISFV N gene

produced results similar to those previously obtained for rVSIV vectors, with and without the expression of a foreign gene, that greatly attenuate vectors both *in vitro* and *in vivo* (35, 40, 41). Genes encoding the VEEV/EEEV E3-E1 proteins were chosen for expression by rISFV vectors because they contain major virus neutralization epitopes (1). The complete E3-E1 polyprotein was expressed from a single rISFV transcription unit in each case to allow natural proteolytic processing, E2/E1 heterodimer folding, and, presumably, authentic structural presentation on the surface of infected cells and rISFV particles. The additional expression cassette was positioned in the fifth position of the rISFV vector in each case to limit the amount of the E3-E1 protein expressed and thereby to reduce the possibility of toxicity to rISFV replication, as has been observed with some other foreign proteins expressed by rVSIV. The highly attenuated rVSIV vector expressing VEEV E3-E1 was based on the rVSIV-N4CT1gag1 vector design, which contains two major attenuating mutations, N gene translocation to genome position 4 (N4) and a truncation of the G protein cytoplasmic tail (CT) from 29 amino acids to a single amino acid (CT1), and has demonstrated safety and immunogenicity in phase I clinical trials (39–42). The attenuation of rISFV vectors may produce lower yields of rISFV-based vaccines; however, strategies have been developed to enhance the yields of highly attenuated rVSIV vectors during good manufacturing practice (GMP) production of clinical trial materials (CTM), and it is very likely that similar strategies can be utilized to overcome any low-yielding rISFV vectors.

Western blot analysis indicated that the level of rISFV-VEEV E3-E1 protein expression was lower than that expressed by rVSIV-VEEV; the reason for this is not clear but could involve reduced transcription initiation efficiency at the ISFV 3' promoter relative to that of VSIV or differences in the attenuation of transcription across intergenic regions. However, a single i.m. dose of either rISFV-VEEV or rISFV-EEEV elicited neutralizing antibody responses and provided complete protection from disease following lethal challenge with VEEV or EEEV, respectively. Complete protection was also observed when both the rISFV-VEEV and rISFV-EEEV vaccine vectors were blended together and administered as a bivalent vaccine formulation, indicating little or no interference between vectors and demonstrating the potential for a multivalent alphavirus vaccine.

Neutralizing antibodies are generally considered to be the correlate of protection against alphavirus infection, and our results are in agreement with data from previous reports. Several studies have suggested the potential role of nonneutralizing antibodies and/or T cell-mediated immunity; however, their role is not well studied or understood (63–66). Consequently, we did not perform analyses of formal correlates of protection and used neutralizing antibody levels as a measure of immunogenicity. Both the rISFV and rVSIV vectors were able to induce neutralizing antibody responses when administered as either a single or a blended regimen. The PRNT₈₀ values were similar when rISFV vectors were administered as single or blended vaccines, although VEEV titers were overall slightly lower when administered as a blended vaccine. The coadministration of multiple alphavirus vaccines can result in interference between vaccine constituents, influencing the immunological readout for each vaccine component, and the very modest reduction in titers observed here may be a reflection of this phenomenon (64, 67–70). The rISFV and rVSIV dose-down study (10⁷ and 10⁸ PFU) indicated that a more durable neutralizing antibody response may be elicited by a higher vaccine dose, but protection from disease was still achieved following challenge at 245 days postvaccination, when neutralizing antibody levels had decreased in the cohort receiving 10⁷ PFU to levels indistinguishable from those in unvaccinated mice, presumably due to the rapid expansion of E3-E1-specific memory B cells after challenge.

The rVSIV-VEEV vector also demonstrated 100% protection of mice from lethal VEEV challenge following a single i.m. vaccine dose. The more robust expression of the VEEV E3-E1 protein observed by Western blot analysis may explain the induction of a greater neutralizing antibody response by rVSIV-VEEV than by rISFV-VEEV, although rVSIV may also be an inherently more immunogenic vector than rISFV.

In summary, we have introduced rISFV as a new vaccine vector platform and demonstrated that rISFV may be attenuated by one of the strategies used for the

attenuation of rVSIV. The attenuated rISFV-VEEV, rISFV-EEEV, and rVSIV-N4CT1 VEEV vectors provided multivalent, single-dose, durable protection of mice from disease following challenge with a lethal dose of EEEV or VEEV. Either of these vectors may provide the pathway to a safe and efficacious vaccine(s) to combat serious disease caused by the encephalitic alphaviruses.

MATERIALS AND METHODS

Viruses and cells. The VSIV San Juan isolate, ISFV, VEEV ZPC 738, and EEEV FL93-939 were obtained from the World Reference Center for Emerging Viruses and Arboviruses at the University of Texas Medical Branch (UTMB).

The Vero cell line was obtained from the American Type Culture Collection (Bethesda, MD). Vero cells were propagated at 37°C with 5% CO₂ in Dulbecco's minimal essential medium (DMEM) containing 10% (vol/vol) fetal bovine serum (FBS), sodium pyruvate (1 mM), 1% (vol/vol) nonessential amino acids, and gentamicin (50 µg/ml).

Phylogenetic analysis. Sequences of the N, G, and L genes were downloaded from GenBank (Table 1) and aligned in SeaView by utilizing the MUSCLE algorithm (71, 72). The sequences were aligned by using the deduced amino acid sequence from open reading frames (ORFs) and then returned to nucleotide sequences for subsequent analyses. Maximum likelihood (ML) analysis was performed by utilizing the PHYLIP package (73). Modeltest in PAUP was used to identify the best-fit nucleotide substitution model, the GTR+I+G model (where GTR is general time reversible, I refers to invariant sites, and G is the gamma distributed rate variation among sites) (74). The robustness of the ML phylogeny was evaluated by bootstrap resampling with 500 replicates.

Generation of rISFV genomic cDNA. An infectious rISFV cDNA clone was generated by amplifying the genome in five DNA fragments flanked by compatible unique restriction enzyme sites (Fig. 2A). The full-length ISFV genome nucleotide sequence was determined from viral RNA isolated from the cell culture supernatant by using the QIAamp viral RNA minikit (Qiagen, Alameda, CA); cDNA for nucleotide sequencing and assembly of a full-length genomic cDNA was generated by reverse transcription (RT) utilizing the Superscript III system (Invitrogen, Carlsbad, CA), using random hexamers. PCR products were generated from this cDNA with Phusion high-fidelity DNA polymerase (NEB) by utilizing ISFV-specific primers. Amplified PCR products were purified by using a QIAquick gel extraction kit (Qiagen) and sequenced by using ABI Prism BigDye Terminator 1.1 cycle sequencing kits, and the reaction products were analyzed on an ABI Prism 3700 DNA analyzer (Invitrogen). Each cDNA fragment was cloned into pBluescript (Invitrogen) in a stepwise manner to generate full-length genomic cDNA. The cDNA nucleotide sequence was verified after each successive round of cloning and after the assembly of a complete genome cDNA, to ensure a match to the viral genome consensus sequence. All full-length cDNA clones and viruses were verified via Sanger sequencing using ABI Prism BigDye Terminator 1.1 cycle sequencing kits on an ABI Prism 3130 or 3700 DNA analyzer (Invitrogen).

Generation of attenuated rISFV and rVSIV vectors. A method for the generation of the highly attenuated rVSIV-N4CT1gag1 vector was described in detail previously (52). By using the rVSIV-N4CT1gag1 cDNA as the starting template, the positions of the N gene and the G_{CT-1} gene were switched, and the expression cassette in position 1, expressing the HIV *gag* gene, was relocated to position 5 between the N and L genes of this vector. These manipulations preserved the N4CT1 attenuating mutations while creating an expression cassette at position 5 for the insertion of the VEEV E2/E1 ORF in place of the *gag* gene. The rISFV genomic cDNA was also manipulated in a similar fashion to translocate the N gene from position 1 to position 4 in the genome, and an expression cassette was then inserted at position 5 between the N and the L genes to accommodate VEEV and EEEV E2/E1 ORFs.

Generation of rISFV and rVSIV vectors expressing alphavirus antigens. As outlined above, cDNA clones of rISFV-N4 and rVSIV-N4CT1 were engineered to contain discrete transcriptional start and stop signals flanked by XhoI and NotI restriction sites, respectively, in the fifth position of the viral genome. The E3-E2-6k-E1 ORFs of the North American-lineage EEEV strain FL93-939 (EEEV-NA) and VEEV subtype ID strain ZPC 738 (VEEV-ID) were inserted into the fifth position of rISFV-N4, and the E3-E2-6k-E1 ORF of VEEV subtype ID was inserted into the fifth position of rVSIV-N4CT1 (Fig. 3).

Vaccine vector nomenclature. Diagrams of rISFV and rVSIV vector genomes are shown in Fig. 3. The positions of N gene and alphavirus E3-E1 ORFs are given relative to those of the wild-type virus genome. The vaccine vectors are referred to throughout the manuscript as rISFV-EEEV (rISFV-N4 EEEV NA FL93-939), rISFV-VEEV (rISFV-N4 VEEV subtype ID strain ZPC 738), rVSIV-HIV (rVSIV-HIVgag5), and rVSIV-VEEV (rVSIV-N4CT1 VEEV subtype ID strain ZPC).

Rescue of rISFV and rVSIV vectors. All rISFV and rVSIV vectors were rescued by electroporation of cDNA plasmids into Vero cells (Fig. 2B). Plasmid DNAs encoding T7 RNA polymerase or rVSIV or rISFV full-length genomic RNA and support plasmids encoding viral N, P, M, G, and L proteins were combined as follows for each electroporation: 50 µg T7, 12 µg genomic cDNA, 12 µg N, 4 µg P, 2 µg M, 2 µg G, and 1 µg L. The plasmid DNA mixture was ethanol precipitated, collected by centrifugation, washed with 70% ethanol, dried, and resuspended in 250 µl of sterile deionized water.

In preparation for electroporation, Vero cells were seeded overnight to obtain ~95% confluent monolayers in a T-150-cm² flask for each electroporation. The monolayers were then trypsinized into single-cell suspensions, followed by the addition of 5 ml of 0.1% (wt/vol) soybean trypsin inhibitor (Invitrogen). Cells were collected by centrifugation and then washed with 20 ml of 1× DMEM containing 10% (vol/vol) fetal bovine serum (FBS), sodium pyruvate (1 mM), 1% (vol/vol) nonessential amino acids, and 0.4% 2-mercaptoethanol (Invitrogen). Cells were collected by centrifugation, resuspended, and

washed in 20 ml of 1× DMEM containing sodium pyruvate (1 mM), 0.4% 2-mercaptoethanol (Invitrogen), 1% (vol/vol) nonessential amino acids, and dimethyl sulfoxide (DMSO) (Corning). Cells were collected by centrifugation and resuspended at $\sim 10^7$ cells per 700 μ l in 1× DMEM containing sodium pyruvate (1 mM), 0.4% 2-mercaptoethanol, 1% (vol/vol) nonessential amino acids, and DMSO. The DNA mixture (250 μ l) and Vero cells (700 μ l) were then mixed by gentle pipetting, and 750 μ l of the mixture was placed into 4-mm electroporation cuvettes and immediately electroporated (BTX, ECM-830 Electro Square Porator; Harvard Apparatus Inc., Holliston, MA). Electroporation was performed at 140 V, the pulse length was 70 ms, the interval between pulses was 500 ms, and the number of pulses was 4. Following electroporation, cells were washed and resuspended in 20 ml of 1× DMEM containing 10% (vol/vol) FBS, sodium pyruvate (1 mM), and 1% (vol/vol) nonessential amino acids. Cells were incubated at 37°C with 5% CO₂ for 3 h, followed by a heat shock at 43°C with 5% CO₂ for 4 h. Following heat shock, cells were placed at 37°C with 5% CO₂, and at 24 h postelectroporation, medium was replaced with Vero cell growth medium. Medium was replaced at 2 days postelectroporation with 1× DMEM containing 2% (vol/vol) FBS, sodium pyruvate (1 mM), 1% (vol/vol) nonessential amino acids, and gentamicin (50 μ g/ml). Flasks were monitored for CPE for 14 days postelectroporation. For each rISFV and rVSIV construct, 6 to 12 electroporation replicates were performed.

Virus propagation, purification, and titration. Virus was routinely amplified and titrated on Vero cell monolayers. For virus amplification, cells were infected at a multiplicity of infection (MOI) of 0.5 PFU/cell. The virus inoculum was adsorbed for 15 min at room temperature, followed by 30 min at 37°C. Additional growth medium was then added, and cells were incubated at 37°C until CPE was observed. The infected cell supernatant was clarified by centrifugation at 3,000 × *g* for 10 min at 4°C. The supernatant was then flash frozen in an ethanol–dry-ice bath and stored at –80°C prior to titration. Virus was further purified from the infected cell supernatant by centrifugation through 10% (wt/vol) sucrose in 1× phosphate-buffered saline (PBS). Briefly, 20 ml of the clarified cell supernatant was underlaid with 14 ml of 10% (wt/vol) sucrose in a Beckmann Ultraclear tube, followed by centrifugation at 28,000 rpm in a Beckmann SW-28 rotor for 1.5 h at 4°C. Following centrifugation, supernatants were aspirated, and the virus pellet was resuspended in PBS and then flash frozen and stored at –80°C prior to plaque assays.

Virus titration was performed on 100% confluent Vero cell monolayers seeded overnight in six-well plates. Duplicate wells were infected with 0.1-ml aliquots of serially 10-fold-diluted virus in growth medium, 0.4 ml of growth medium was also added to each well to prevent cell desiccation, and virus was adsorbed for 15 min at room temperature and then for 30 min at 37°C. Following adsorption, the virus inoculum was aspirated, and cell monolayers were overlaid with 3 ml of 0.4% (wt/vol) Sea-Plaque agarose (Cambrex Bio Science) in growth medium. After 10 min at room temperature to allow the agarose to set, cells were incubated at 32°C with 5% CO₂ for 1 to 3 days to allow plaque development. Following incubation, the overlay was removed, and cells were stained with 2% crystal violet in 70% methanol for 5 min at room temperature; excess stain was removed under running water, and plaques were counted.

One-step growth kinetics. Virus growth kinetics were assessed on 100% confluent Vero cell monolayers seeded overnight in T-25-cm² tissue culture flasks. Virus infections were performed in triplicate at an MOI of 10 PFU/cell, and virus was adsorbed for 15 min at room temperature, followed by 30 min at 37°C. Following incubation, the inoculum was removed, monolayers were rinsed five times with room-temperature DMEM to remove any unbound virus, and 5 ml of growth medium was added to each flask; 0.5-ml samples were taken immediately afterwards, designated “T 0” samples, and replaced with 0.5 ml of fresh medium. Flasks were incubated at 37°C, and additional samples were taken at 6, 9, 12, 24, and 48 hpi. All samples were flash frozen in ethanol-dry ice and stored at –80°C.

Western blotting. Replicate confluent Vero cell monolayers in six-well plates were infected at an MOI of 5 PFU per cell. The virus inoculum was adsorbed for 15 min at room temperature, followed by 30 min at 37°C. Additional growth medium was then added, and cells were incubated at 37°C under 5% CO₂ for 24 h. At 24 hpi, cells were scraped into the suspension and collected by centrifugation at 3,000 × *g* for 10 min at 4°C. The supernatant was removed, and cell pellets were treated with 0.5 ml of lysis buffer (0.05 M Tris-HCl [pH 7.5], 0.01 M NaCl, 1× Triton X-100). Cell lysates were then diluted 1:1 in Laemmli sample buffer (Bio-Rad) and heated at 90°C for 5 min to denature proteins. Samples were electrophoresed on 4 to 12% Bis-Tris-polyacrylamide gel electrophoresis gels (NuPAGE) with a Precision Plus protein standard (Bio-Rad), and proteins were then transferred onto a nitrocellulose membrane by using the iBlot system (Invitrogen). Mouse polyclonal antisera against VEEV and EEEV were obtained from the World Reference Center for Emerging Viruses and Arboviruses at the University of Texas Medical Branch. Antisera were diluted 1:1,000 in diluent provided in the Western Breeze anti-mouse chromogenic kit (Invitrogen). Color was allowed to develop after the addition of a chromogenic substrate provided in the Western Breeze kit, and the nitrocellulose membrane was then rinsed with distilled H₂O and air dried.

Plaque reduction neutralization test. Serum samples were heat inactivated at 56°C for 30 min. Samples were serially diluted 2-fold in a solution containing DMEM, 2% FBS, and gentamicin (50 μ g/ml); mixed with an equal volume of 2,000 PFU/ml of VEEV ZPC or EEEV FL93; and incubated for 1 h at 37°C. Vero cell monolayers in 6-well plates were then inoculated with 100 μ l of the serum-virus mixture in triplicate. Anti-VEEV- or EEEV-positive sera, and medium-only controls, and virus-only controls were included in the assay. Plates were incubated at 37°C with 5% CO₂ for 3 days and then fixed and stained with crystal violet as described above. PRNT₈₀ values were calculated and expressed as the reciprocal of the serum dilution yielding a >80% reduction (PRNT₈₀) in the number of plaques.

Mouse vaccination and challenge. All studies were carried out in accordance with the recommendations in the *Guide for the Care and Use of Laboratory Animals* of the National Institutes of Health and were approved by Institutional Animal Care and Use Committee protocol 02-09-068 at UTMB (75). CD-1 outbred female mice, 4 to 6 weeks old, from Charles River (Wilmington, MA) were utilized in the studies.

Mice received 10^8 or 10^7 PFU of either the rVSV or rISFV vaccine vector in 50 μ l of PBS by i.m. injection. Vaccinated mice were challenged with a lethal dose (10^4 PFU) of either VEEV-ID or EEEV-NA by s.c. injection. Based on the outcome of the first pilot EEEV vaccine study, mice were subsequently challenged with 10^5 PFU by i.p. injection. Mice were observed daily for signs of illness and were euthanized with the onset of neurological disease, consistent with previous VEEV and EEEV challenge studies (76, 77).

Statistics. RStudio (version 0.97; RStudio, Boston, MA) running R (version 3.0.1; R Development Core Team, Vienna, Austria) software was used for statistical analysis. Significant differences in mean titers between wt viruses and attenuated vaccine constructs were determined by using two-way analysis of variance (ANOVA) for all viruses, followed by a Tukey test. A two-tailed Fisher exact test was performed to determine significant differences in survival rates.

ACKNOWLEDGMENTS

This work was supported by National Institutes of Health grant AI120942.

F.N., D.M., R.L.S., T.L., R.V.G., R.M.N., S.H., J.H.E., R.B.T., D.K.C., and S.C.W. have a patent pending on an Isfahan virus vaccine platform.

The views expressed in this article are those of the authors and do not reflect the official policy or position of the U.S. Department of Defense or the Department of the Army.

REFERENCES

- Knipe DM, Howley PM, Cohen JI, Griffin DE, Lamb RA, Martin MA, Racaniello VR, Roizman B (ed). 2013. *Fields virology*, 6th ed, vol 1. Lippincott Williams & Wilkins, Philadelphia, PA.
- Tesh RB, Travassos Da Rosa AP, Travassos Da Rosa JS. 1983. Antigenic relationship among rhabdoviruses infecting terrestrial vertebrates. *J Gen Virol* 64(Part 1):169–176.
- Tesh R, Saidi S, Javadian E, Loh P, Nadim A. 1977. Isfahan virus, a new vesiculovirus infecting humans, gerbils, and sandflies in Iran. *Am J Trop Med Hyg* 26:299–306.
- Gaidamovich S, Obukhova VR, Sveshnikova NA, Cherednichenko IUN, Kostiuokov MA. 1978. Natural foci of viruses borne by *Phlebotomus papatasi* in the USSR according to a serologic study of the population. *Vopr Virusol* 1978:556–560. (In Russian.)
- Gaidamovich S, Altukhova LM, Obukhova VR, Ponirovskii EN, Sadykov VG. 1980. Isolation of the Isfahan virus in Turkmenia. *Vopr Virusol* 1980:618–620. (In Russian.)
- Wilks CR, House JA. 1986. Susceptibility of various animals to the vesiculoviruses Isfahan and Chandipura. *J Hyg (Lond)* 97:359–368. <https://doi.org/10.1017/S002217240006544X>.
- Cotton WE. 1926. The causal agent of vesicular stomatitis proved to be a filter-passing virus. *J Am Vet Med Assoc* 23:168–179.
- Letchworth GJ, Rodriguez LL, Del Cbarrera J. 1999. Vesicular stomatitis. *Vet J* 157:239–260. <https://doi.org/10.1053/tvj.1998.0303>.
- Johnson KM, Vogel JE, Peralta PH. 1966. Clinical and serological response to laboratory-acquired human infection by Indiana type vesicular stomatitis virus (VSV). *Am J Trop Med Hyg* 15:244–246.
- Fields BN, Hawkins K. 1967. Human infection with the virus of vesicular stomatitis during an epizootic. *N Engl J Med* 277:989–994. <https://doi.org/10.1056/NEJM196711092771901>.
- Ball LA, White CN. 1976. Order of transcription of genes of vesicular stomatitis virus. *Proc Natl Acad Sci U S A* 73:442–446. <https://doi.org/10.1073/pnas.73.2.442>.
- Ge P, Tsao J, Schein S, Green TJ, Luo M, Zhou ZH. 2010. Cryo-EM model of the bullet-shaped vesicular stomatitis virus. *Science* 327:689–693. <https://doi.org/10.1126/science.1181766>.
- Emerson SU, Yu Y. 1975. Both NS and L proteins are required for in vitro RNA synthesis by vesicular stomatitis virus. *J Virol* 15:1348–1356.
- Emerson SU, Wagner RR. 1972. Dissociation and reconstitution of the transcriptase and template activities of vesicular stomatitis B and T virions. *J Virol* 10:297–309.
- Abraham G, Banerjee AK. 1976. Sequential transcription of the genes of vesicular stomatitis virus. *Proc Natl Acad Sci U S A* 73:1504–1508. <https://doi.org/10.1073/pnas.73.5.1504>.
- Schnell MJ, Mebatsion T, Conzelmann KK. 1994. Infectious rabies viruses from cloned cDNA. *EMBO J* 13:4195–4203.
- Lawson ND, Stillman EA, Whitt MA, Rose JK. 1995. Recombinant vesicular stomatitis viruses from DNA. *Proc Natl Acad Sci U S A* 92:4477–4481. <https://doi.org/10.1073/pnas.92.10.4477>.
- Whelan SP, Ball LA, Barr JN, Wertz GT. 1995. Efficient recovery of infectious vesicular stomatitis virus entirely from cDNA clones. *Proc Natl Acad Sci U S A* 92:8388–8392. <https://doi.org/10.1073/pnas.92.18.8388>.
- Schnell MJ, Buonocore L, Whitt MA, Rose JK. 1996. The minimal conserved transcription stop-start signal promotes stable expression of a foreign gene in vesicular stomatitis virus. *J Virol* 70:2318–2323.
- Chattopadhyay A, Wang E, Seymour R, Weaver SC, Rose JK. 2013. A chimeric vesiculo/alphavirus is an effective alphavirus vaccine. *J Virol* 87:395–402. <https://doi.org/10.1128/JVI.01860-12>.
- Cobleigh MA, Buonocore L, Uprichard SL, Rose JK, Robek MD. 2010. A vesicular stomatitis virus-based hepatitis B virus vaccine vector provides protection against challenge in a single dose. *J Virol* 84:7513–7522. <https://doi.org/10.1128/JVI.00200-10>.
- Kahn JS, Roberts A, Weibel C, Buonocore L, Rose JK. 2001. Replication-competent or attenuated, nonpropagating vesicular stomatitis viruses expressing respiratory syncytial virus (RSV) antigens protect mice against RSV challenge. *J Virol* 75:11079–11087. <https://doi.org/10.1128/JVI.75.22.11079-11087.2001>.
- Kapadia SU, Rose JK, Lamirande E, Vogel L, Subbarao K, Roberts A. 2005. Long-term protection from SARS coronavirus infection conferred by a single immunization with an attenuated VSV-based vaccine. *Virology* 340:174–182. <https://doi.org/10.1016/j.virol.2005.06.016>.
- Matassov D, Marzi A, Latham T, Xu R, Ota-Setlik A, Feldmann F, Geisbert JB, Mire CE, Hamm S, Nowak B, Egan MA, Geisbert TW, Eldridge JH, Feldmann H, Clarke DK. 2015. Vaccination with a highly attenuated recombinant vesicular stomatitis virus vector protects against challenge with a lethal dose of Ebola virus. *J Infect Dis* 212(Suppl 2):S443–S451. <https://doi.org/10.1093/infdis/jiv316>.
- Mire CE, Matassov D, Geisbert JB, Latham TE, Agans KN, Xu R, Ota-Setlik A, Egan MA, Fenton KA, Clarke DK, Eldridge JH, Geisbert TW. 2015. Single-dose attenuated Vesiculovax vaccines protect primates against Ebola Makona virus. *Nature* 520:688–691. <https://doi.org/10.1038/nature14428>.
- Natuk RJ, Cooper D, Guo M, Calderon P, Wright KJ, Nasar F, Witko S, Pawlyk D, Lee M, DeStefano J, Tummolo D, Abramovitz AS, Gangolli S, Kalyan N, Clarke DK, Hendry RM, Eldridge JH, Udem SA, Kowalski J. 2006. Recombinant vesicular stomatitis virus vectors expressing herpes simplex virus type 2 gD elicit robust CD4⁺ Th1 immune responses and are protective in mouse and guinea pig models of vaginal challenge. *J Virol* 80:4447–4457. <https://doi.org/10.1128/JVI.80.9.4447-4457.2006>.
- Palin A, Chattopadhyay A, Park S, Delmas G, Suresh R, Senina S, Perlin DS, Rose JK. 2007. An optimized vaccine vector based on recombinant vesicular stomatitis virus gives high-level, long-term protection against *Yersinia pestis* challenge. *Vaccine* 25:741–750. <https://doi.org/10.1016/j.vaccine.2006.08.010>.
- Roberts A, Kretzschmar E, Perkins AS, Forman J, Price R, Buonocore L, Kawaoka Y, Rose JK. 1998. Vaccination with a recombinant vesicular stomatitis virus expressing an influenza virus hemagglutinin provides complete protection from influenza virus challenge. *J Virol* 72:4704–4711.

29. Roberts A, Reuter JD, Wilson JH, Baldwin S, Rose JK. 2004. Complete protection from papillomavirus challenge after a single vaccination with a vesicular stomatitis virus vector expressing high levels of L1 protein. *J Virol* 78:3196–3199. <https://doi.org/10.1128/JVI.78.6.3196-3199.2004>.
30. Rose NF, Marx PA, Luckay A, Nixon DF, Moretto WJ, Donahoe SM, Montefiori D, Roberts A, Buonocore L, Rose JK. 2001. An effective AIDS vaccine based on live attenuated vesicular stomatitis virus recombinants. *Cell* 106:539–549. [https://doi.org/10.1016/S0092-8674\(01\)00482-2](https://doi.org/10.1016/S0092-8674(01)00482-2).
31. Schwartz JA, Buonocore L, Roberts A, Suguitan A, Jr, Kobasa D, Kobinger G, Feldmann H, Subbarao K, Rose JK. 2007. Vesicular stomatitis virus vectors expressing avian influenza H5 HA induce cross-neutralizing antibodies and long-term protection. *Virology* 366:166–173. <https://doi.org/10.1016/j.virol.2007.04.021>.
32. Frank AH, Appleby A, Seibold HR. 1945. Experimental intracerebral infection of horses, cattle, and sheep with the virus of vesicular stomatitis. *Am J Vet Res* 6:28–38.
33. Sabin AB, Olitsky PK. 1938. Influence of host factors on neuroinvasiveness of vesicular stomatitis virus. IV. Variations in neuroinvasiveness in different species. *J Exp Med* 67:229–249.
34. Wagner RR. 1974. Pathogenicity and immunogenicity for mice of temperature-sensitive mutants of vesicular stomatitis virus. *Infect Immun* 10:309–315.
35. Wertz GW, Perepelitsa VP, Ball LA. 1998. Gene rearrangement attenuates expression and lethality of a nonsegmented negative strand RNA virus. *Proc Natl Acad Sci U S A* 95:3501–3506. <https://doi.org/10.1073/pnas.95.7.3501>.
36. Levenbuk IS, Nikolayeva MA, Chigirinsky AE, Ralf NM, Kozlov VG, Vardanyan NV, Sliopushkina VG, Kolomiets OL, Rukhamina ML, Grigoryeva LV. 1979. On the morphological evaluation of the neurovirulence safety of attenuated mumps virus strains in monkeys. *J Biol Stand* 7:9–19. [https://doi.org/10.1016/S0092-1157\(79\)80033-5](https://doi.org/10.1016/S0092-1157(79)80033-5).
37. Rubin SA, Snoy PJ, Wright KE, Brown EG, Reeve P, Beeler JA, Carbone KM. 1999. The mumps virus neurovirulence safety test in rhesus monkeys: a comparison of mumps virus strains. *J Infect Dis* 180:521–525. <https://doi.org/10.1086/314905>.
38. Johnson JE, Nasar F, Coleman JW, Price RE, Javadian A, Draper K, Lee M, Reilly PA, Clarke DK, Hendry RM, Udem SA. 2007. Neurovirulence properties of recombinant vesicular stomatitis virus vectors in non-human primates. *Virology* 360:36–49. <https://doi.org/10.1016/j.virol.2006.10.026>.
39. Clarke DK, Nasar F, Chong S, Johnson JE, Coleman JW, Lee M, Witko SE, Kotash CS, Abdullah R, Megati S, Luckay A, Nowak B, Lackner A, Price RE, Little P, Kalyan N, Randolph V, Javadian A, Zamb TJ, Parks CL, Egan MA, Eldridge J, Hendry M, Udem SA. 2014. Neurovirulence and immunogenicity of attenuated recombinant vesicular stomatitis viruses in nonhuman primates. *J Virol* 88:6690–6701. <https://doi.org/10.1128/JVI.03441-13>.
40. Clarke DK, Nasar F, Lee M, Johnson JE, Wright K, Calderon P, Guo M, Natuk R, Cooper D, Hendry RM, Udem SA. 2007. Synergistic attenuation of vesicular stomatitis virus by combination of specific G gene truncations and N gene translocations. *J Virol* 81:2056–2064. <https://doi.org/10.1128/JVI.01911-06>.
41. Cooper D, Wright KJ, Calderon PC, Guo M, Nasar F, Johnson JE, Coleman JW, Lee M, Kotash C, Yurgeloni I, Natuk RJ, Hendry RM, Udem SA, Clarke DK. 2008. Attenuation of recombinant vesicular stomatitis virus-human immunodeficiency virus type 1 vaccine vectors by gene translocations and G gene truncation reduces neurovirulence and enhances immunogenicity in mice. *J Virol* 82:207–219. <https://doi.org/10.1128/JVI.01515-07>.
42. Fuchs JD, Frank I, Elizaga ML, Allen M, Frahm N, Kochar N, Li S, Edupuganti S, Kalams SA, Tomaras GD, Sheets R, Pensiero M, Tremblay MA, Higgins TJ, Latham T, Egan MA, Clarke DK, Eldridge JH, HVTN 090 Study Group and the National Institutes of Allergy and Infectious Diseases HIV Vaccine Trials Network, Mulligan M, Roupheal N, Estep S, Rybczyk K, Dunbar D, Buchbinder S, Wagner T, Isbell R, Chinnell V, Bae J, Escamilla G, Tseng J, Fair R, Ramirez S, Broder G, Briesemeister L, Ferrara A. 2015. First-in-human evaluation of the safety and immunogenicity of a recombinant vesicular stomatitis virus human immunodeficiency virus-1 gag vaccine (HVTN 090). *Open Forum Infect Dis* 2:ofv082. <https://doi.org/10.1093/ofid/ofv082>.
43. Forrester NL, Palacios G, Tesh RB, Savji N, Guzman H, Sherman M, Weaver SC, Lipkin WI. 2012. Genome-scale phylogeny of the alphavirus genus suggests a marine origin. *J Virol* 86:2729–2738. <https://doi.org/10.1128/JVI.05591-11>.
44. Nasar F, Palacios G, Gorchakov RV, Guzman H, Da Rosa AP, Savji N, Popov VL, Sherman MB, Lipkin WI, Tesh RB, Weaver SC. 2012. Eilat virus, a unique alphavirus with host range restricted to insects by RNA replication. *Proc Natl Acad Sci U S A* 109:14622–14627. <https://doi.org/10.1073/pnas.1204787109>.
45. La Linn M, Gardner J, Warrilow D, Darnell GA, McMahon CR, Field I, Hyatt AD, Slade RW, Suhrbier A. 2001. Arbovirus of marine mammals: a new alphavirus isolated from the elephant seal louse, *Lepidophthirus macrorhini*. *J Virol* 75:4103–4109. <https://doi.org/10.1128/JVI.75.9.4103-4109.2001>.
46. Villoing S, Bearzotti M, Chilmoneczyk S, Castric J, Bremont M. 2000. Rainbow trout sleeping disease virus is an atypical alphavirus. *J Virol* 74:173–183. <https://doi.org/10.1128/JVI.74.1.173-183.2000>.
47. Weston JH, Welsh MD, McLoughlin MF, Todd D. 1999. Salmon pancreas disease virus, an alphavirus infecting farmed Atlantic salmon, *Salmo salar* L. *Virology* 256:188–195. <https://doi.org/10.1006/viro.1999.9654>.
48. Reed DS, Lackemeyer MG, Garza NL, Norris S, Gamble S, Sullivan LJ, Lind CM, Raymond JL. 2007. Severe encephalitis in cynomolgus macaques exposed to aerosolized Eastern equine encephalitis virus. *J Infect Dis* 196:441–450. <https://doi.org/10.1086/519391>.
49. Reed DS, Larsen T, Sullivan LJ, Lind CM, Lackemeyer MG, Pratt WD, Parker MD. 2005. Aerosol exposure to Western equine encephalitis virus causes fever and encephalitis in cynomolgus macaques. *J Infect Dis* 192:1173–1182. <https://doi.org/10.1086/444397>.
50. Reed DS, Lind CM, Sullivan LJ, Pratt WD, Parker MD. 2004. Aerosol infection of cynomolgus macaques with enzootic strains of Venezuelan equine encephalitis viruses. *J Infect Dis* 189:1013–1017. <https://doi.org/10.1086/382281>.
51. Clarke DK, Sidhu MS, Johnson JE, Udem SA. 2000. Rescue of mumps virus from cDNA. *J Virol* 74:4831–4838. <https://doi.org/10.1128/JVI.74.10.4831-4838.2000>.
52. Witko SE, Kotash CS, Nowak RM, Johnson JE, Boutilier LA, Melville KJ, Heron SG, Clarke DK, Abramovitz AS, Hendry RM, Sidhu MS, Udem SA, Parks CL. 2006. An efficient helper-virus-free method for rescue of recombinant paramyxoviruses and rhadoviruses from a cell line suitable for vaccine development. *J Virol Methods* 135:91–101. <https://doi.org/10.1016/j.jviromet.2006.02.006>.
53. Aguilar PV, Adams AP, Wang E, Kang W, Carrara AS, Anishchenko M, Frolov I, Weaver SC. 2008. Structural and nonstructural protein genome regions of Eastern equine encephalitis virus are determinants of interferon sensitivity and murine virulence. *J Virol* 82:4920–4930. <https://doi.org/10.1128/JVI.02514-07>.
54. Anishchenko M, Paessler S, Greene IP, Aguilar PV, Carrara AS, Weaver SC. 2004. Generation and characterization of closely related epizootic and enzootic infectious cDNA clones for studying interferon sensitivity and emergence mechanisms of Venezuelan equine encephalitis virus. *J Virol* 78:1–8. <https://doi.org/10.1128/JVI.78.1.1-8.2004>.
55. Ahmed M, McKenzie MO, Puckett S, Hojnacki M, Poliquin L, Lyles DS. 2003. Ability of the matrix protein of vesicular stomatitis virus to suppress beta interferon gene expression is genetically correlated with the inhibition of host RNA and protein synthesis. *J Virol* 77:4646–4657. <https://doi.org/10.1128/JVI.77.8.4646-4657.2003>.
56. Carroll AR, Wagner RR. 1979. Role of the membrane (M) protein in endogenous inhibition of in vitro transcription by vesicular stomatitis virus. *J Virol* 29:134–142.
57. Clinton GM, Little SP, Hagen FS, Huang AS. 1978. The matrix (M) protein of vesicular stomatitis virus regulates transcription. *Cell* 15:1455–1462. [https://doi.org/10.1016/0092-8674\(78\)90069-7](https://doi.org/10.1016/0092-8674(78)90069-7).
58. Conzelmann KK. 2005. Transcriptional activation of alpha/beta interferon genes: interference by nonsegmented negative-strand RNA viruses. *J Virol* 79:5241–5248. <https://doi.org/10.1128/JVI.79.9.5241-5248.2005>.
59. Dubovi EJ, Wagner RR. 1977. Spatial relationships of the proteins of vesicular stomatitis virus: induction of reversible oligomers by cleavable protein cross-linkers and oxidation. *J Virol* 22:500–509.
60. Ferran MC, Lucas-Lenard JM. 1997. The vesicular stomatitis virus matrix protein inhibits transcription from the human beta interferon promoter. *J Virol* 71:371–377.
61. Jayakar HR, Jeetendra E, Whitt MA. 2004. Rhabdovirus assembly and budding. *Virus Res* 106:117–132. <https://doi.org/10.1016/j.virusres.2004.08.009>.
62. Saidi S, Tesh R, Javadian E, Sahabi Z, Nadim A. 1977. Studies on the epidemiology of sandfly fever in Iran. II. The prevalence of human and

- animal infection with five phlebotomus fever virus serotypes in Isfahan province. *Am J Trop Med Hyg* 26:288–293.
63. Schmaljohn AL, Johnson ED, Dalrymple JM, Cole GA. 1982. Non-neutralizing monoclonal antibodies can prevent lethal alphavirus encephalitis. *Nature* 297:70–72. <https://doi.org/10.1038/297070a0>.
64. Reed DS, Glass PJ, Bakken RR, Barth JF, Lind CM, da Silva L, Hart MK, Rayner J, Alterson K, Custer M, Dudek J, Owens G, Kamrud KI, Parker MD, Smith J. 2014. Combined alphavirus replicon particle vaccine induces durable and cross-protective immune responses against equine encephalitis viruses. *J Virol* 88:12077–12086. <https://doi.org/10.1128/JVI.01406-14>.
65. Reed DS, Lind CM, Lackemeyer MG, Sullivan LJ, Pratt WD, Parker MD. 2005. Genetically engineered, live, attenuated vaccines protect nonhuman primates against aerosol challenge with a virulent IE strain of Venezuelan equine encephalitis virus. *Vaccine* 23:3139–3147. <https://doi.org/10.1016/j.vaccine.2004.12.023>.
66. Roy CJ, Adams AP, Wang E, Leal G, Seymour RL, Sivasubramani SK, Mega W, Frolov I, Didier PJ, Weaver SC. 2013. A chimeric Sindbis-based vaccine protects cynomolgus macaques against a lethal aerosol challenge of Eastern equine encephalitis virus. *Vaccine* 31:1464–1470. <https://doi.org/10.1016/j.vaccine.2013.01.014>.
67. Reisler RB, Gibbs PH, Danner DK, Boudreau EF. 2012. Immune interference in the setting of same-day administration of two similar inactivated alphavirus vaccines: Eastern equine and Western equine encephalitis. *Vaccine* 30:7271–7277. <https://doi.org/10.1016/j.vaccine.2012.09.049>.
68. Cole FE, Jr, McKinney RW. 1971. Cross-protection in hamsters immunized with group A arbovirus vaccines. *Infect Immun* 4:37–43.
69. Calisher CH, Sasso DR, Sather GE. 1973. Possible evidence for interference with Venezuelan equine encephalitis virus vaccination of equines by pre-existing antibody to Eastern or Western equine encephalitis virus, or both. *Appl Microbiol* 26:485–488.
70. Pittman PR, Liu CT, Cannon TL, Mangiafico JA, Gibbs PH. 2009. Immune interference after sequential alphavirus vaccine vaccinations. *Vaccine* 27:4879–4882. <https://doi.org/10.1016/j.vaccine.2009.02.090>.
71. Edgar RC. 2004. MUSCLE: multiple sequence alignment with high accuracy and high throughput. *Nucleic Acids Res* 32:1792–1797. <https://doi.org/10.1093/nar/gkh340>.
72. Gouy M, Guindon S, Gascuel O. 2010. SeaView version 4: a multiplatform graphical user interface for sequence alignment and phylogenetic tree building. *Mol Biol Evol* 27:221–224. <https://doi.org/10.1093/molbev/msp259>.
73. Felsenstein J. 1989. PHYLIP—Phylogeny Inference Package (version 3.2). *Cladistics* 5:164–166.
74. Posada D, Crandall KA. 1998. MODELTEST: testing the model of DNA substitution. *Bioinformatics* 14:817–818. <https://doi.org/10.1093/bioinformatics/14.9.817>.
75. National Research Council. 2011. Guide for the care and use of laboratory animals, 8th ed. National Academies Press, Washington, DC.
76. Pandya J, Gorchakov R, Wang E, Leal G, Weaver SC. 2012. A vaccine candidate for Eastern equine encephalitis virus based on IRES-mediated attenuation. *Vaccine* 30:1276–1282. <https://doi.org/10.1016/j.vaccine.2011.12.121>.
77. Rossi SL, Guerbois M, Gorchakov R, Plante KS, Forrester NL, Weaver SC. 2013. IRES-based Venezuelan equine encephalitis vaccine candidate elicits protective immunity in mice. *Virology* 437:81–88. <https://doi.org/10.1016/j.virol.2012.11.013>.